Pharmacological modulation of dopamine receptors reveals distinct brain-wide networks associated with learning and motivation in non-human primates.

Atsushi Fujimoto[1,2#]*, Catherine Elorette[1,2#], Satoka H. Fujimoto[1,2], Lazar Fleysher[5], Peter H. Rudebeck[1,2+], and Brian E. Russ[1,3,4+]*

Author affiliations:

[1] Nash Family Department of Neuroscience and Friedman Brain Institute, Icahn School of Medicine at Mount Sinai, One Gustave L. Levy Place, New York, NY 10029

[2] Lipschultz Center for Cognitive Neuroscience, Icahn School of Medicine at Mount Sinai, New York, NY, 10029

[3] Center for Biomedical Imaging and Neuromodulation, Nathan Kline Institute, 140 Old Orangeburg Road, Orangeburg, NY 10962

[4] Department of Psychiatry, New York University at Langone, One, 8, Park Ave, New York, NY 10016

[5] BioMedical Engineering and Imaging Institute, Icahn School of Medicine at Mount Sinai, One Gustave L. Levy Place, New York, NY 10029

[#] These authors contributed equally to this work

[+] Joint last author

*** Correspondence:**

Atsushi Fujimoto and Brian E. Russ

atsushi.fujimoto@mssm.edu or brian.russ@nki.rfmh.org

Short title: Dopaminergic networks for learning and motivation

Abstract

The neurotransmitter dopamine (DA) has a multifaceted role in healthy and disordered brains through its action on multiple subtypes of dopaminergic receptors. How modulation of these receptors influences learning and motivation by altering intrinsic brain-wide networks remains unclear. Here we performed parallel behavioral and resting-state functional MRI experiments after administration of two different DA receptor antagonists in macaque monkeys. Systemic administration of SCH-23390 (D1 antagonist)

slowed probabilistic learning when subjects had to learn new stimulus-reward associations and diminished functional connectivity (FC) in cortico-cortical and fronto-striatal connections. By contrast, haloperidol (D2 antagonist) improved learning and broadly enhanced FC in cortical connections. Further comparisons between the effect of SCH-23390/haloperidol on behavioral and resting-state FC revealed specific cortical and subcortical networks associated with the cognitive and motivational effects of DA manipulation, respectively. Thus, we reveal distinct brain-wide networks that are associated with the dopaminergic control of learning and motivation via DA receptors.

Significance Statement

D1 and D2 receptors are heavily implicated in cognitive and motivational processes, as well as in a number of psychiatric disorders. Despite this, little is known about how selective manipulation of these different receptors impacts cognition through changing activity across brain-wide intrinsic networks. Here, we examined the acute behavioral and brain-wide effects of D1 and D2 receptor-selective antagonists, SCH-23390 and haloperidol, in macaques performing a probabilistic learning task. SCH administration diminished, and haloperidol improved, animals' task performance. Mirroring these effects on behavior, SCH reduced, and haloperidol increased, the resting-state functional connectivity across brain-wide networks, most notably in the cortico-striatal areas. Thus, our results highlight the opposing effects of D1 and D2 receptor modulation on the brain and behavior.

Introduction

Dopamine (DA), a neurotransmitter in the central nervous system, plays a critical role in learning, cognitive control, and working memory as well as motivated behavior (Brozoski et al., 1979; Schultz et al., 1997; Volkow et al., 1998; Robbins and Everitt, 2002; Remy and Samson, 2003; Noudoost and Moore, 2011; Ott and Nieder, 2019). DA acts through its binding to various dopamine receptors that are heterogeneously distributed across the brain (Seeman, 1987; Self, 2010). The dopamine D1 and D2 receptors are the most prevalent subtypes of dopamine receptors in both humans and animals and they are heavily implicated in psychiatric conditions such as schizophrenia (Lidow et al., 1998; Brisch et al., 2014).

Extensive research has found that D1 and D2 receptors have distinct roles in learning and motivation. D1 receptor blockade through systemic or local administration in prefrontal cortex disrupts cue-reward association learning and probabilistic reversal learning in rats, while blocking of D2 receptors promotes learning (Eyny and Horvitz, 2003; Zeeb et al., 2009; St Onge et al., 2011; Jenni et al., 2021). Similarly, in macaque monkeys, local administration of a D1 antagonist, SCH-23390, into dorsolateral prefrontal cortex impairs working memory and learning (Sawaguchi and Goldman-Rakic, 1991; Puig and Miller, 2012). By contrast, systemic administration of the D2 antagonist haloperidol, which is widely used to ameliorate positive symptoms of schizophrenia (Settle and Ayd, 1983; Adams et al., 2013), facilitated value discounting (Hori et al., 2021). At the same time, drugs that impact D1 and D2 receptors have differential effects on neural activity. Specifically, earlier PET and SPECT studies reported that the D2 antagonist haloperidol increases cerebral blood flow in healthy individuals and in clinically responsive schizophrenia patients (Buchsbaum et al., 1992; Goldman et al., 1996). Resting-state fMRI studies reported a decrease in the hemodynamic response following administration of D1 antagonist SCH-23390 in rats (Choi et al., 2006), while D2 antagonist haloperidol, or agonist bromocriptine, enhanced dorsal fronto-parietal networks in healthy human subjects (Cole et al., 2013; Vogelsang et al., 2023). Although these studies provided partial evidence as to how D1 and D2 modulation impacts brain-wide intrinsic MRI functional connectivity, how higher doses that are sufficient to robustly modulate behavior would impact brain-wide networks remains unclear.

To address these issues, we conducted parallel behavioral and resting-state functional neuroimaging experiments in macaque monkeys. We found that the selective D1 and D2 receptor antagonists, SCH-23390 and haloperidol respectively (Beaulieu and Gainetdinov, 2011), induced contrasting effects on both behavior and functional connectivity in whole-brain networks. Further, the cortical functional connectivity changes induced by DA antagonists were correlated with task performance, especially when subjects had to learn new stimulus-reward associations. Thus, our results reveal the brain-wide impact of selectively manipulating activity at different DA receptor subtypes, shedding light on the neural networks that are associated with dopamine receptor-dependent cognitive function.

Materials and Methods

Subjects

Seven rhesus macaques (*Macaca mulatta*, 7-8 years old, 4 females) served as subjects. All subjects were pair or grouped-housed, were maintained on a 12-h light/dark cycle and had access to food 24 hours a day. During training and testing each subject's access to water was controlled for 5 days per week. The

experiments performed for each subject are summarized in **Table 1**. All procedures were approved by the Icahn School of Medicine Animal Care and Use Committee.

Surgery

Prior to training, an MRI compatible head-fixation device (Rogue research, Montréal, Canada) was surgically implanted using dental acrylic (Lang Dental, Wheeling, IL) and ceramic screws (Thomas Research Products, Elgin, IL) in the animals that underwent behavioral testing (monkeys Ee, Me, Pi, St). In a dedicated operating suite using aseptic procedures, anesthesia was induced using ketamine (10 mg/kg, i.m.) and then maintained by isoflurane (2-3%). The skin, fascia, and muscles were opened and retracted. 8-10 MR-compatible ceramic screws were implanted into the cranium and the head fixation device was bonded to the screws using dental acrylic. The muscles, fascia, and skin were then sutured closed. The animals were treated with dexamethasone sodium phosphate (0.4 mg/kg, i.m.) and cefazolin antibiotic (15 mg/kg, i.m.) for one day before and one week after surgery. After surgery and for two additional days, the animals received ketoprofen analgesic (10-15 mg/kg, i.m.); ibuprofen (100 mg) was administered for five additional days and all postoperative medications were given in consultation with veterinary staff. The position of implant was determined based on a pre-acquired T1-weighted MR image.

Drugs

SCH-23390 hydrochloride (Tocris Bioscience, Minneapolis, MN) and haloperidol (Sigma-Aldrich, St. Louis, MO) were used as our D1 and D2 receptor selective antagonists, respectively. Both SCH and haloperidol were dissolved and diluted in 0.9% saline to achieve the target dose within 1 ml solution. 0.9% saline (1 ml) was also used as a control solution. The solution was prepared fresh on every experimental day using sterile procedures.

Behavioral experiments

A probabilistic learning task was developed for macaque monkeys (**Fig. 1A**). The task was controlled by NIMH MonkeyLogic software (Hwang et al., 2019) running on MATLAB 2019a (MathWorks, Natick, MA) and presented on a monitor in front of the monkey. In this task, animals were required to choose, using an eye movement, between two visual stimuli presented on either side of a monitor. A trial began with appearance of a fixation spot (white cross) at the center of the screen. The monkey had to acquire and maintain fixation for 1-1.5 sec to initiate a trial. The fixation spot was extinguished, and two visual stimuli were simultaneously presented to the right and left on the screen. The two stimuli presented on each trial were randomly chosen from a larger pool of three visual stimuli that were associated with different reward probabilities (0.9, 0.5, and 0.3) (**Fig. 1B**). Each trial therefore fell into three categories based on the reward probabilities of the options presented: High-Low (0.9-0.3), High-Mid (0.9-0.5), and Mid-Low (0.5-0.3). Stimuli were either novel at the beginning of each block of 100 trials (novel block) or subjects had previously learned about the reward-probability associated with each image and were highly familiar with them (familiar block). Once stimuli were presented, subjects were required to move their eyes toward either right or left stimulus option (‘response’) within 2 seconds. Following a response, the chosen stimulus remained on screen for 0.3 sec and then was removed, and a fluid reward was then immediately delivered based on the probability of the chosen option. Subsequently an inter-trial interval (ITI, 3-3.5 sec) followed. A trial with a fixation break during the fixation period or with no response within the response window was aborted; all stimuli were extinguished immediately, and an ITI started. The same trial was repeated following an aborted trial.

The animals performed 4-6 blocks in which the novel or familiar stimuli were pseudorandomly interleaved in hour-long sessions. The monkeys were trained for 3-6 months before behavioral experiments with drug injections or resting-state fMRI scans. The I.M. injection of saline, SCH-23390 (10, 30, or 50 µg/kg), or haloperidol solution (5 or 10 µg/kg) was performed 15 minutes prior to the task start. Each monkey completed at least 3 sessions at each dose level for each drug for a total of 80-138 total blocks per monkey. The order of treatment was randomized, and injections were at least a day (SCH-23390) or week apart (haloperidol) to avoid potential prolonged effects of the drug, in accordance with known pharmacokinetics of the drugs in macaque monkeys (Hori et al., 2021).

Resting-state fMRI data acquisition

The scans were performed under the same protocol we previously developed for macaque monkeys (Fujimoto et al., 2022; Elorette et al., 2024). In brief, following sedation with ketamine (5mg/kg) and dexmedetomidine (0.0125mg/kg) the animals were intubated. They were then administered (i.v.) monocrystalline iron oxide nanoparticle or MION (10 mg/kg, BioPAL, Worcester, MA), and three EPI functional scans (1.6 mm isotropic, TR/TE 2120/16 ms, flip angle 45°, 300 volumes per each run) were obtained, along with a T1-weighted structural scan (0.5 mm isotropic, MPRage TR/TI/TE 2500/1200/3.27 ms, flip angle 8°) (pre-injection scans). Following drug i.v. injection (saline, SCH-23390, or haloperidol) and 15 minutes waiting period, another set of three functional scans was acquired (post-injection scans). Low-level isoflurane (0.7-0.9%) was used to maintain sedation through a session so that neural activity was preserved while minimizing motion artifacts. Vital signs (end-tidal CO_2, body temperature, blood pressure, capnograph) were continuously monitored and maintained as steadily as possible throughout an experimental session. The doses of drugs used in the scans (50 µg/kg and 10 µg/kg for SCH and haloperidol, respectively) were pre-determined based on a prior PET study to achieve up to 70-80% occupancy of the DA receptors in macaques (Hori et al., 2021).

Behavioral data analyses

All behavioral data was analyzed using MATLAB 2019a. Choice performance was defined as the proportion of trials in a block (100 trials) in which monkeys chose an option associated with higher reward probability in the stimulus pair presented. Response time (RT) was defined as the duration from the timing of visual stimuli presentation to the timing of response initiation. Choice performance was computed for bins of 10 trials at each block and averaged for each subject, then finally averaged across subjects for each block type. We reasoned that a significant interaction ($p < 0.05$) of trial bin by block type with 2-way repeated measures ANOVA (trial bin: 1-10 × block type: novel or familiar) indicated that there was an improvement in performance due to successful learning in novel blocks but not in familiar blocks. Choice performance and RT on each stimulus pair in the latter half of each block were assessed by 1-way repeated-measures ANOVA (stimulus pair: 0.9-0.3, 0.9-0.5, 0.5-0.3) for each block type in saline sessions. The effect of SCH-23390 or haloperidol injection on choice performance and RT was assessed by 3-way repeated-measures ANOVA (block type: novel or familiar × stimulus pair: 0.9-0.3, 0.9-0.5, 0.5-0.3 × drug dose: 0, 10, 30, 50 µg/kg SCH-23390, and 0, 5, or 10 µg/kg haloperidol). To further assess the effects of drugs on each block type, we also performed 2-way repeated-measures ANOVA (stimulus pair: 0.9-0.3, 0.9-0.5, 0.5-0.3 × drug dose: 0, 10, 30, 50 µg/kg for SCH-23390, and 0, 5, or 10 µg/kg for haloperidol, respectively). All multi-way ANOVA was performed by using MATLAB built-in function *anovan* with monkeys modeled as a random effect.

We also performed a model fitting analysis for the choice data in novel blocks employing a standard reinforcement learning model with a softmax choice function (Sutton and Barto, 1981; Rudebeck et al., 2017b) described as below:

$$V_{i(t+1)} = V_{i(t)} + \alpha \times \left(R_{(t)} - V_{i(t)}\right) \quad (1)$$

$$P_{i(t)} = \frac{exp(\beta \times V_i)}{\sum_{j=1}^{3} exp(\beta \times V_j)} \quad (2)$$

Where α and β represent learning rate and inverse temperature, respectively. $V_{i(t)}$ and $R_{(t)}$ indicate the value of the chosen option *i* and outcome on trial *t*. $P_{i(t)}$ indicates the choice probability of option *i* on trial *t*. Then the log-likelihood (LL) and the Bayesian Information Criterion (BIC) were calculated for each block to assess how well the model fitted the data:

$$LL = \sum_{t=1}^{T} \log \sum_{j=1}^{3} C_{j(t)} P_{j(t)} \quad (3)$$

$$BIC = -2 \log T - k \times LL \quad (4)$$

Where *T* and *k* denote the size of trial block and the number of parameters, respectively. $C_{j(t)} = 1$ when the subject chooses option *j* in trial *t*, and $C_{j(t)} = 0$ for all unchosen options. The learning rate and inverse temperature were estimated using MATLAB function *fminsearchbnd* to select parameters by minimizing the log-likelihood function for each block. The best-fit parameters were averaged for each drug condition, and the dose-dependent effects of drugs as well as BIC were assessed by 1-way repeated-measures ANOVA (drug dose: 0, 10, 30, 50 μg/kg for SCH-23390, and 0, 5, or 10 μg/kg for haloperidol, respectively).

fMRI data analysis

The detail of preprocessing steps for functional imaging data was described in our previous study (Fujimoto et al., 2022). In brief, all functional imaging data was initially converted to NIFTI format and preprocessed with custom AFNI/SUMA pipelines (Cox, 1996; Jung et al., 2021; Fujimoto et al., 2022). The T1 weighted image from each session was skullstripped (Wang et al., 2021) and then warped to the standard NMT atlas space (Seidlitz et al., 2018). The EPI data were further preprocessed using a customized version of the AFNI NHP preprocessing pipeline (Jung et al., 2021). The first 3 TRs of each EPI were removed to eliminate any magnetization effects. Then, the images went through slice timing correction, motion correction, alignment to T1w image, warping to standard space, blurring, and then converted to percent signal change. Finally, motion derivatives from each scan along with CSF and WM signals were regressed and the residuals of this analysis were used in the following analysis.

The functional connectivity (FC) analysis was performed using 3dNetCorr function in AFNI (Cox, 1996; Taylor and Saad, 2013). The regions of interest (ROIs) were defined based on the cortical hierarchical atlas (CHARM) (Jung et al., 2021) and subcortical hierarchical atlas (SARM) (Hartig et al., 2021) for rhesus macaques, both at level 4. The matrices of FC across all ROI pairs, or connectomes, were Fisher's z-transformed for each session, and the pre-injection connectome was subtracted from post-injection connectome. Then, the connectomes representing the drug-induced change in FC (ΔFC) were averaged within treatment conditions (SCH-23390, haloperidol, saline). To statistically determine the effects, the ΔFCs derived from each ROI were averaged and compared to a null distribution ($\alpha = 0.05$ with Bonferroni's correction, rank-sum test). The connectomes were also visualized in the circular plot with the threshold set at $z = 0.1$ (absolute value) created using the circularGraph toolbox run in MATLAB (Kassebaum, 2023). Separately, we also analyzed the whole-brain FC using a dorsal and ventral striatum seed. Correction for multiple comparisons was performed using 3dClustSim, which computed the cluster-size threshold based on 10000 iteration of Monte Carlo simulations in AFNI (Cox, 1996). The combination of initial thresholding at $p < 0.01$ and the cluster-size threshold at 6 voxels corresponds to corrected $p < 0.05$.

The relationship between the connectome and behavioral data (correct performance and RT) and between the connectome and RL parameters (learning rate and inverse temperature) were analyzed on the data where ΔFC and behavioral data were obtained under the same drug condition, and all drug conditions (saline, SCH, haloperidol) were combined. The correlation analysis was performed separately for each functional connection or ROI pair, and a matrix of correlation coefficients (R) was created. A permutation test was performed for each functional connection by comparing R^2 computed from real data and that derived from shuffled data with randomized behavioral sessions 1000 times. The correlation matrix was also projected into a brain map of macaque monkeys by connecting the center of each ROI with a line reflecting the R-value and sign (positive or negative) of correlation as the line width and color, respectively. For visualization purposes the fraction of connections that showed strong behavior-ΔFC correlation (top 5%) were plotted. The R values in the matrix were averaged across functional connections for each of cortico-cortical, cortico-subcortical, and subcortico-subcortical ROI pairs and compared to the null distribution (rank-sum test).

Results

Distinct effects of dopamine receptor antagonists on probabilistic stimulus-reward learning

Four macaque monkeys were trained to perform a probabilistic learning task for fluid rewards. On each trial, the animals were free to choose between the two visual stimuli by making an eye movement to obtain a juice reward (**Fig. 1A**). The stimuli presented on each trial were randomly chosen from a set of three stimuli that were associated with distinct reward probabilities (0.9, 0.5, and 0.3) (**Fig. 1B**). Subjects completed 100-trial blocks with either stimuli that were novel at the start of each block (novel blocks) or that they had previously learned (familiar blocks).

In novel blocks with saline administration, monkeys gradually learned to discriminate between the different stimuli (**Fig. 1C**). By contrast, in the familiar blocks subjects reliably maintained a high and stable performance throughout a given block, suggesting memory-guided choices (**Fig. 1E**). A two-way repeated-measures ANOVA (trial bin: 1-10 × block type: novel or familiar) revealed a significant interaction of trial bin by block type on choice performance ($p < 0.01$, $F_{(9,1097)} = 8.0$), confirming the difference between novel and familiar blocks. Subjects' choice performance was also influenced by which stimuli were presented as options on each trial. A one-way repeated-measures ANOVA (stimulus pair: 0.9-0.3, 0.9-0.5, 0.5-0.3) revealed a significant main effect of stimulus pair on choice performance in both novel and familiar blocks (novel blocks: $p < 0.01$, $F_{(2,168)} = 16.3$; familiar blocks: $p < 0.01$, $F_{(2,153)} = 15.3$, **Fig. 1C and E**). Additionally, response time (RT) reflected the reward probability of available options in both block types, such that RT was shorter for trials in which the high reward probability stimulus was presented (one-way repeated-measures ANOVA, novel blocks: $p = 0.027$, $F_{(2,168)} = 3.7$; familiar blocks: $p < 0.01$, $F_{(2,153)} = 53.8$, main effect of stimulus pair, **Fig. 1D and F**). Importantly, the patterns of behavior were consistent across all subjects in both the novel and familiar blocks (**Fig. 1C-F**).

Following administration of dopamine receptor antagonists, behavioral performance was impacted (**Fig. 2A and B**). A set of larger ANOVA models including both SCH-23390 and haloperidol conditions (drug × block type × stimulus pair) revealed a significant interaction of drug by block type ($p < 0.01$, $F_{(5,1110)} = 3.6$), indicating that dopamine receptor antagonists specifically impact performance when monkeys have to learn novel stimulus-reward associations. Notably, we found that SCH-23390

tended to decrease subjects' performance in novel blocks ($p = 0.061$, $F_{(3,441)} = 2.5$, main effect of drug dose, 2-way repeated-measures ANOVA), while it did not affect the performance in blocks with familiar stimuli ($p = 0.90$, $F_{(3,399)} = 0.20$) (**Fig. 2C**). The treatment also affected RT such that higher doses of SCH increased RT in both novel and familiar blocks (novel blocks: $p < 0.01$, $F_{(3,441)} = 24.0$; familiar blocks: $p = 0.015$, $F_{(3,399)} = 3.5$) (**Fig. 2D**). In contrast to SCH-23390, haloperidol increased subjects' correct performance in novel blocks ($p = 0.037$, $F_{(2,342)} = 3.3$), while it did not affect the performance in familiar blocks ($p = 0.63$, $F_{(2,309)} = 0.46$) (**Fig. 2E**). Notably, administration of haloperidol did not affect subjects RTs in either novel or familiar blocks ($p > 0.53$), suggesting negligible effects on monkeys' motivation at the range of doses we used (**Fig. 2F**). Thus, dopamine receptor antagonists induced opposing effects on learning novel probabilistic stimulus-reward associations at the higher doses that we used, while they had no discernable impact on familiar associations.

We also assessed the effect of drugs during learning by a model fitting analysis employing a standard two parameter reinforcement learning model (see Materials and Methods). The model was fitted to the animals' choice data in each block of the novel condition (**Fig. 3A**), and the average of best-fit parameters were computed for each drug condition (**Fig. 3B-C**). This analysis revealed that haloperidol, but not SCH-23390 administration, tended to decrease inverse temperature (haloperidol: $p = 0.073$, $F_{(2,110)} = 2.7$, SCH-23390: $p = 0.81$, $F_{(3,141)} = 0.32$, main effect of drug dose with 1-way repeated-measures ANOVA), while neither drug changed the animals' learning rate ($p > 0.20$). Importantly, we did not find a significant difference between the model fits as measured by the Bayesian Information Criteria (BIC), across the different levels of SCH-23390 or haloperidol ($p > 0.25$, main effect of drug dose with 1-way repeated-measures ANOVA). This result indicates that D2 receptor manipulation impacted the animals' degree of exploration, while D1 receptor antagonism did not affect either process, during learning.

Contrasting effects of dopamine receptor antagonists on fronto-striatal functional connectivity

Given the clear differences between D1 and D2 receptor antagonism on monkeys' performance of the probabilistic task, we next set out to determine which networks might be most influenced by our two DA receptor antagonists and therefore potentially driving the behavioral effects. To do this we analyzed resting-state functional images that were obtained in parallel to the behavioral experiments. In addition to the cohort that completed behavioral testing detailed above, three other macaques also underwent saline scans to serve as additional baseline data for our analyses (see **Table 1**).

First, to assess the effects of the drugs on an area known to be high in D1 and D2 receptors that has also been implicated in associative learning (Balleine et al., 2007; Clarke et al., 2008; Vo et al., 2014; White and Monosov, 2016), we analyzed the change in dorsal striatum functional connectivity (FC) induced by administration of either SCH-233980 or haloperidol. During baseline imaging, before the injection of either drug, signal in the dorsal striatum ROI (SARM atlas) (Hartig et al., 2021) exhibited high levels of correlation with frontal cortex, including parts of ventrolateral prefrontal cortex (vlPFC) and orbitofrontal cortex (OFC) (**Fig. 4A**). As expected, injection of saline had little effect on dorsal striatum FC with the rest of the brain (**Fig. 4B**). By contrast, administration of SCH-23390 induced broad changes in dorsal striatum FC (**Fig. 4C**). Notably, D1-receptor antagonism specifically

decreased dorsal striatum FC with OFC and lateral prefrontal cortex, while increasing correlations within the dorsal striatum itself ($p < 0.05$, cluster-level correction). By contrast, administration of haloperidol significantly increased FC in frontal-striatal circuits, most notably between striatum and parts of the medial OFC and vlPFC ($p < 0.05$, **Fig. 4D**), while showing minimal change in FC within the dorsal striatum. We also analyzed the drug effects on the whole-brain FC using the ventral striatum as the seed ROI (SARM level 4 atlas), as this part of the striatum is also implicated in reinforcement learning (van der Meer and Redish, 2011; Averbeck and Costa, 2017) (**Fig. 4E-H**). We found that SCH-23390 and haloperidol induced FC changes similar to those we observed in dorsal striatum, although both the baseline FC and the effects of the drugs were relatively small and there were no significant drug-induced changes in connectivity with frontal cortex ($p > 0.05$, cluster-level correction). Thus, D1 and D2 receptor antagonism appears to have opposing effects on dorsal striatum FC in macaques, especially with the parts of frontal cortex involved in probabilistic learning (Rudebeck et al., 2017a; Murray and Rudebeck, 2018).

Functional connectome analysis reveals distinct network signatures associated with dopamine receptor antagonism

To further characterize the impact of the D1 and D2 receptor antagonists on brain-wide networks, we performed atlas-based full connectome analyses. Here we used pre-determined anatomical ROIs from the cortical and subcortical atlas of the macaque monkey (CHARM and SARM atlas, respectively) (Hartig et al., 2021; Jung et al., 2021) and normalized FCs (z-value) were computed for all ROI pairs to produce connectomes. The pre-injection connectomes were similar to those reported previously (Grayson et al., 2016; Fujimoto et al., 2022) (**Fig. 5A, left column**). As expected, injections of saline were not associated with systematic changes in FCs (ΔFCs) of the cortical and subcortical connectome (**Fig. 5A, top row**). By contrast, SCH-23390 injection induced an overall decrease in FCs primarily between cortical regions (**Fig. 5A, middle row**), whereas haloperidol injection induced the opposite pattern of effects on FCs (**Fig. 5A, bottom row**). Indeed, the average z-value for each pair of ROIs showed contrasting effects overall, where SCH-23390 decreased and haloperidol increased FC between cortical sites ($p < 0.05$ with Bonferroni correction, rank-sum test, **Fig. 5B**).

We further visualized the changes in FC following injections of SCH-23390 or haloperidol by projecting the ΔFC connectomes onto circular plots (absolute difference in z-value > 0.1, **Fig. 5C**). This approach revealed unique patterns of network-level effects induced by SCH-23390 and haloperidol. Specifically, SCH-23390 was associated with a general decrease in cortico-cortical FC in frontal and temporal areas, fronto-striatal FC, and meso/thalamo-cortical FCs. In contrast, haloperidol primarily caused an increase in cortico-cortical FC in frontal, parietal, and temporal areas as well as fronto-striatal FC. In addition to increased FCs, some connections such as midbrain to parietal cortex FC were decreased by treatment with haloperidol. Overall, mirroring our earlier behavioral analyses, SCH-23390 and haloperidol induced contrasting effects in brain-wide FCs, and in particular induced opposite effects in fronto-striatal and cortico-cortical FCs.

Network correlates of behavioral performance associated with dopaminergic function

The prior analysis shows that the behavioral effects of D1 and D2 receptor antagonism are associated with distinct changes in brain-wide FC. To directly compare behavioral and neuroimaging datasets, we next examined whether the pharmacologically induced changes in resting-state functional connectivity (ΔFC) are related to the effects on behavioral data, either correct performance or RT, that were obtained after the administration of matching doses of the same D1- and D2-antagonists. This allowed us to assess whether changes in FC were related to changes in behavioral responses during a task, even though they were tested under different settings.

We first chose several areas known to be involved in probabilistic learning, namely OFC, vlPFC, dorsal and ventral striatum, mediodorsal thalamus, and midbrain (Clarke et al., 2008; Rudebeck et al., 2017a; Murray and Rudebeck, 2018), and specifically analyzed functional connectivity between those structures. Notably, we found that dorsal striatum-to-OFC ΔFC was significantly correlated with the correct performance in novel blocks ($p < 0.01$, $r = 0.32$) (**Fig. 6A and B**), while there was no association between performance in the familiar blocks ($p = 0.96$) or RTs ($p > 0.38$) (**Fig. 6C**). The same pattern was seen between OFC-to-12m/o (rostral vlPFC) ΔFC and behavior where a positive correlation was observed between the FC changes and the performance in the novel block ($p < 0.01$, $r = 0.34$) (**Fig. 6D-F**). This result indicates that these connections may be involved specifically in learning rather than in the probabilistic choice in general. By contrast, we found a distinct effect on connectivity between mediodorsal thalamus and caudal vlPFC (area 12o): ΔFC between these structures showed no significant correlation with the animals' performance during the novel blocks ($p = 0.79$, $r = 0.03$), but there was a significant negative correlation with performance during the familiar blocks ($p = 0.016$, $r = -0.30$) (**Fig. 6G and H**). However, ΔFC between these regions was related to subject's RTs in both conditions (novel blocks: $p < 0.01$, $r = -0.45$; familiar blocks: $p < 0.01$, $p = -0.41$) (**Fig. 6I**). Similarly, ventral striatum-to-midbrain ΔFC was also related to RT effects in both conditions ($p < 0.032$) and showed no significant association with correct performance ($p > 0.074$) (**Fig. 6J-L**). The strong negative correlation observed between ΔFC and the animals' RTs suggests that these connections are involved in functions such as motivation or motor control.

Next, we extended the approach described above on the full connectome of all ROI pairs and measures of behavior (**Fig. 7**). **Figure 7A** depicts the functional connections where we observed a strong correlation between ΔFC and task performance. The brain map indicates that the task performance in novel blocks was positively correlated to cortico-cortical and cortico-subcortical ΔFCs (**Fig. 7A, left**). Interestingly, the pattern was strikingly different when we analyzed the familiar block; strong correlations were observed mainly in subcortical regions, while cortico-cortical ΔFCs were less correlated to the performance (**Fig. 7A, right**). The full correlation matrix further revealed the detail of these differences (**Fig. 7C**). Notably, there was a strong correlation between correct performance and ΔFCs in cortical areas including frontal, parietal, and temporal regions, as well as in these regions' functional connections to striatum in the novel blocks (**Fig. 7C, left**). A permutation test with shuffled behavioral sessions (1000 iterations) confirmed that the correlations in those functional connections were significantly greater than the chance (> 95% confidence interval, **Fig. 7E**).

In the familiar blocks, the correlations between cortical areas and performance were less strong, although the change in some functional connections, involving midbrain and thalamic areas as well as sensory and motor cortex, were strongly correlated to the performance (**Fig. 7C, right**). Consequently,

when we averaged connections based on their link between cortical and subcortical ROIs (cortico-cortical, cortico-subcortical, and subcortico-subcortical), we found a distinct pattern of connections that showed strong correlation to task performance in each block type ($p < 0.01$, $F_{(2,15000)} = 68.1$, interaction of area category by block type, 2-way ANOVA) (**Fig. 7G**). Subsequent post-hoc analysis revealed that the cortico-cortical and cortico-subcortical behavior-ΔFC correlations were higher in the novel blocks compared to familiar blocks ($p < 0.01$, Tukey-Kramer test), while the relationship between subcortico-subcortical ΔFC and behavioral performance was lower in novel blocks and higher in familiar blocks ($p < 0.01$) (**Fig. 7G**).

We performed a similar analysis between ΔFC and RT across novel and familiar blocks (**Fig. 7B and D**). Here we observed a negative correlation between behavior and ΔFC in cortical areas but a positive correlation between behavior and ΔFC in midbrain and thalamic connections in both novel and familiar blocks (**Fig. 7F and H**). Although there was a significant interaction of area category by block type ($p < 0.01$, $F_{(2,15000)} = 4.6$) there was no significant difference in subcortico-subcortical connections ($p = 1.0$, Tukey-Kramer test). This suggests that RT was associated with subcortical FC in a similar manner in both blocks. Interestingly, the pattern of correlation between RT and ΔFC was similar to that with task performance in familiar blocks (**Fig. 7C and D**). This result suggests that the brain-wide networks associated with learning novel associations that are modulated by dopaminergic antagonists are largely separable from those associated with memory-based choices to familiar stimuli or response times. We also conducted the same analysis with behavioral data normalized for each subject (z-transformed). The networks correlated to each behavior matched those shown in **Figure 7**; cortico-cortical and cortico-subcortical behavior-ΔFC correlations were higher in the novel blocks compared to familiar blocks and subcortico-subcortical behavior-ΔFC correlations were lower in novel blocks than that in familiar blocks ($p < 0.01$, Tukey-Kramer test). No significant difference in subcortico-subcortical connections was observed in the relationship between the RT and ΔFC ($p = 0.40$).

Finally, we performed a correlation analysis between ΔFC and RL model parameters that were computed by fitting the animals' choice data in novel blocks with a standard two-parameter RL model (**Fig. 3**). Because our model fitting analysis showed a selective change in inverse temperature following haloperidol, we expected to observe a stronger correlation between ΔFC and inverse temperature than that between ΔFC and learning rate. As predicted, ΔFC showed a strong and negative correlation to inverse temperature (> 95% confidence interval), while their correlation to learning rate was less pronounced (**Fig. 8A-C**). Strong correlations were observed in cortico-cortical and cortico-subcortical connections preferentially with inverse temperature (**Fig. 8D,** $p < 0.01$, $F_{(2,15000)} = 46.4$, interaction of area category by RL parameter, 2-way ANOVA), which mirrored the pattern observed when we analyzed correlation between ΔFC and performance in novel blocks (**Fig. 7G**), suggesting an overlap of the circuits associated with the degree of exploration and learning performance.

In sum, our analysis directly correlating behavior and resting-state FC changes induced by dopaminergic receptor antagonists revealed distinct neural networks that were associated with specific behavioral domains.

Discussion

Here we conducted concurrent behavioral and resting-state fMRI experiments in macaque monkeys to assess the impact of dopamine D1 and D2 receptor antagonists on the brain-wide networks that support learning and motivation. Administration of the D1 receptor antagonist SCH-23390 reduced performance on a probabilistic learning task and reduced resting-state FC in cortico-cortical and fronto-striatal networks. By contrast, administration of the D2 receptor antagonist haloperidol improved performance on the same task and increased FC in cortical networks. When we looked for relationships between behavior and changes in FC induced by D1/D2 antagonists, we found that effects of dopaminergic manipulation related to learning were associated with cortico-cortical connections, whereas the effect on motivational aspects of task performance were associated with subcortical FC. Taken together, our results identified distinct brain-wide networks that underlie the impact of D1 and D2 antagonists on learning and motivation.

The role of D1 and D2 receptors in learning and memory-based choices

The effects of DA receptor manipulation on behavior have been extensively studied in both humans and animals. Past reports using rats or macaques showed that the administration of D1 antagonist SCH-23390 and D2 antagonists raclopride or haloperidol induced opposing effects in reward-based learning and probabilistic choices (Sawaguchi and Goldman-Rakic, 1991; Eyny and Horvitz, 2003; Zeeb et al., 2009; St Onge et al., 2011; Puig and Miller, 2012; Hori et al., 2021; Jenni et al., 2021). Interestingly, unlike the robust behavioral effects observed in past studies using animal subjects, relatively mixed effects of D2 antagonism were reported in the studies using healthy humans as subjects. For instance, several studies reported that D2 antagonism enhanced reward-related signals in healthy human subjects (Jocham et al., 2011; Kahnt et al., 2015; Clos et al., 2019). In contrast, other studies reported that D2 antagonists lacked a clear effect on exploration/exploitation behaviors in a reinforcement learning task (Chakroun et al., 2020) or even impaired reinforcement learning by disrupting reward prediction error signaling (Pessiglione et al., 2006; Eisenegger et al., 2014; Diederen et al., 2017). These differences could be derived from individual variability in baseline dopamine levels (Cools and D'Esposito, 2011) and the choice of the dose given to participants (Chakroun et al., 2020), or due to dose-dependent difference in the main site of action of haloperidol (i.e., pre-synaptic vs. post-synaptic effects), as we discuss later. In addition, there is a possibility that the difference in task design across studies could lead to such a discrepancy in the drug's effect on the overall choice performance. In the human studies that observed deficits in performance following haloperidol treatment, subjects performed two-option probabilistic tasks (Pessiglione et al., 2006; Eisenegger et al., 2014). By contrast, in the current study subjects chose between three stimuli that were probabilistically rewarded in each novel block, which likely made value-based learning harder and favored more prolonged exploration. Thus, it is possible that increasing the degree of exploration was advantageous in our task but was actually disadvantageous in the two-option tasks. Indeed, fitting a two-parameter reinforcement learning model to the subjects' choices showed that haloperidol selectively decreased the inverse temperature parameter in novel blocks. Notably, this change in the degree of exploration was consistent with the above human studies even though the effect on correct performance was the opposite. This highlights that the haloperidol dose that we used here did not simply change subjects' performance via modulating motivation or attention, but specifically impacted their behavioral strategies including the degree of exploration. Additionally, our

task design tested animals in both novel and familiar conditions, allowing us to dissociate the behavioral effects of drugs on learning from those on motor or motivational functions.

Our behavioral results were overall consistent with the existing literature; D1 antagonist SCH impaired and D2 antagonist haloperidol facilitated the performance of our monkeys in novel blocks (**Fig. 2**). Notably, DA receptor manipulation in this range did not affect the performance in the familiar block, suggesting that the actions of DA through D1 and D2 receptors play a specific role in new association learning rather than choices in general. In addition to the effects on learning performance, we also observed a change in subjects' RTs specifically in the SCH sessions. Notably the impact of SCH on RT was observed in both novel and familiar blocks, suggesting that the effect of DA receptor manipulation on motivation or motor function is dissociable from the effects on learning. Our model fitting analysis further revealed a selective and dose-dependent decrease in the inverse temperature parameter following administration of the D2 receptor antagonist haloperidol, suggesting that this improved the animals' performance by slightly increasing the level of exploration. The negative effect of D2 antagonism on the inverse temperature parameter without appreciably impacting the learning rate is consistent to previous findings in human subjects (Pessiglione et al., 2006; Eisenegger et al., 2014). Taken together, our behavioral analyses demonstrated contrasting behavioral effects following systemic manipulation of D1 and D2 receptors, where D2 receptor antagonism specifically impacted choice consistency during learning.

It is important to note, however, that the effect of haloperidol administration on behavior could be interpreted as being predominantly caused by its affinity for pre-synaptic D2 receptors on striatal neurons. On this view, haloperidol at low doses could inhibit pre-synaptic D2 receptors, which is thought to lead to increased DA release from the axon terminal. If this was the case, the effects of haloperidol administration in our experiments would be the result of increased DA release as opposed to haloperidol antagonistically acting on post-synaptic D2 receptors. Indeed, the doses we used in the current study were lower than the doses typically used in human studies or in clinical settings where more than 1-2 mg haloperidol (equivalent to 14-28 ug/kg for a 70 kg male subject) was used (Pessiglione et al., 2006; Chakroun et al., 2020). There are several reasons why we believe that this is unlikely to be the case. First, our haloperidol dosage was determined based on a prior PET study using drug-naïve macaques, where single administration of 10 ug/kg haloperidol occupied 80% of striatal D2 receptors (Hori et al., 2021). By contrast, in healthy humans, single administration of 3 mg (42 ug/kg for a 70 kg male) haloperidol occupies only 35-65% of D2 receptors in the striatum (Ishiwata et al., 2006; Lim et al., 2013). Notably, daily treatment with 3 mg haloperidol leads to 80% D2 occupancy after several days in humans (Zipursky et al., 2005; Lako et al., 2013; Lim et al., 2013). In addition to this, there appear to be differences between effective doses of haloperidol across species that must be considered when comparing studies of humans and animal models (Kapur et al., 2000; Mukherjee et al., 2001). Therefore, it is likely that our haloperidol doses were not low in terms of D2 receptor occupancy level, and that their administration to drug-naïve macaques sufficiently induced post-synaptic effects that are equivalent to the previous human studies. We acknowledge, however, that without further investigation with higher doses of haloperidol, and/or additional investigation using dopamine agonists, we cannot rule out the possibility that our haloperidol results are at least partially accounted for by its action to pre-synaptic D2 receptors. Future study should delineate among these possibilities by testing both agonists and antagonists in wider dose ranges.

Dopaminergic modulation of fMRI resting-state functional connectivity

Previous studies have mainly analyzed neural effects of DA receptor manipulation by focusing on specific areas such as prefrontal cortex and striatum (Wang et al., 2004; Noudoost and Moore, 2011; Puig and Miller, 2012; Yael et al., 2013; Puig and Miller, 2015; Kunimatsu and Tanaka, 2016). One advantage of our resting-state fMRI approach is that it can identify drug effects on intrinsic networks free from the indirect impact of drug-induced behavioral changes. Further, our neuroimaging protocol uses a low level of anesthesia to preserve resting-state FC in macaque monkeys meaning that brain-wide FC patterns are still sensitive to pharmacological treatment (Fujimoto et al., 2022; Elorette et al., 2024). Using this approach, our whole-brain connectome analyses revealed contrasting effects of SCH and haloperidol, particularly in cortico-cortical and cortico-subcortical connections, mirroring the changes in learning performance induced by the same drugs (**Fig. 5**). In addition to the known effects on fronto-striatal circuits and fronto-parietal networks, diverse cortical regions including temporal areas and thalamic nuclei were involved. The present results highlight that large-scale functional networks are recruited by DA receptor modulation to influence various cognitive and motor functions.

Interestingly, the pattern of effects on functional connectivity after D2 receptor manipulation did not simply reflect the known distribution of this receptor subtype within the primate brain, which is mainly localized to the striatum (Suhara et al., 1999; Tsukada et al., 2005; Froudist-Walsh et al., 2021; Hori et al., 2021). It is unlikely that the non-specific binding of haloperidol to D1 receptors caused changes in cortical areas, as the overall direction of the effects was the opposite between those drug conditions. One possibility is that the haloperidol induced substantial neural changes through interactions with D2 receptors expressed in cortical neurons, including presynaptic autoreceptors (Beaulieu and Gainetdinov, 2011; Cools and D'Esposito, 2011). Indeed, previous studies demonstrated that cortical D2 receptors are functionally relevant (Narendran et al., 2009; Narendran et al., 2014) and associated with positive symptoms in schizophrenia (Suhara et al., 2002; Mizrahi et al., 2007), although the profile of cortical D2 receptors is still unclear due to technical limitations (Tritsch and Sabatini, 2012). This question could be addressed by recording neuronal activity from D1 and D2 receptor expressing neurons in both cortical and striatal regions.

Dissociable neural networks for distinct dopamine-dependent behaviors

Past studies have demonstrated that resting-state FC can be used to predict the behavioral effects of pharmacological treatments on learning, memory recall, and attention, in both humans and macaques (Li et al., 2013; Kohno et al., 2014; Fujimoto et al., 2022). Our within-subject behavior-connectivity correlation analysis revealed distinct brain networks where connectivity was correlated with task performance or RT (**Fig. 7**). The network that we identified related to learning performance included fronto-striatal and fronto-parietal circuits and largely overlaps with networks known to be more active when subjects are learning reward-based associations (Cools et al., 2004; Cohen, 2008; Chadick and Gazzaley, 2011; Frank and Badre, 2012; Sescousse et al., 2013; Gilmore et al., 2015). Further correlation analysis between the connectome and RL parameters revealed that these brain networks are associated with variation in the inverse temperature, suggesting that the dopamine receptor manipulation

predominantly affects the degree of exploration rather than the rate of value updating. It is noteworthy that the network reflecting task performance in familiar blocks, including midbrain and thalamic nuclei, largely overlaps with the network of brain areas correlated with RT. That different behavioral domains engaged the same network of areas indicates that this system may play a central role in motivation or motor control of executing a choice after learning has occurred. Indeed, a recent study demonstrated that silencing of the ventral tegmental area to ventral striatum pathway in macaques affected motivation but did not impair reinforcement learning (Vancraeyenest et al., 2020). Thus, our analysis revealed distinct neural networks where dopamine takes action to modulate behaviors in primates.

Conclusion

Dopaminergic signaling, especially an optimal balance between D1 and D2 receptor-dependent modulation, is critical for normal learning (Seeman, 1987; Takahashi et al., 2012), and its alteration may contribute to the basis of schizophrenia (Sedvall and Karlsson, 1999; Yun et al., 2023). The similarity of the dopaminergic system between non-human primates and humans (Berger et al., 1991; Raghanti et al., 2008) means that our findings have implications for the brain-wide actions of antipsychotics in humans. Thus, our data provide evidence that the cognitive effects of D1/D2 receptor modulation are related to altered functional connections among cortical areas and reveal a possible mechanism through which systemic pharmacological DA receptor manipulation contributes to ameliorating aberrant cognition.

Acknowledgments: A.F., C.E., B.E.R., and P.H.R. are supported by grants from the BRAIN initiative (R01MH117040). B.E.R. is supported by grants from NIMH (R01MH111439) and NINDS (R01NS109498). A.F. is supported by Overseas Research Fellowship from Takeda Science Foundation and a Brain & Behavior Research Foundation Young Investigator grant (#28979). We would like to thank Dr. Paula Croxson for providing the foundation on which this work was built, Dr. Yukiko Hori for advising on drug preparation, and Jairo Munoz and Niranjana Bienkowska for assistance with data acquisition. For help with fMRI data pre-processing and analysis we thank Drs Paul Taylor and Alex Franco, respectively. We also thank Drs. Jacqueline-Marie Ferland, Dan Iosifescu, and Takafumi Minamimoto for their comments on the earlier version of the manuscript.

Conflict of interest: The authors declare no competing financial interest.

Author contributions: A.F. designed the study. A.F. and C.E. collected the behavioral data. A.F., C.E., S.H.F., and L.F. collected the imaging data. A.F. analyzed the data. A.F., C.E., P.H.R., and B.E.R. wrote the original draft. All authors edited the paper.

Data Availability: The data that support the findings of this study are available from the corresponding authors upon reasonable request.

References

Adams CE, Bergman H, Irving CB, Lawrie S (2013) Haloperidol versus placebo for schizophrenia. Cochrane Database of Systematic Reviews.

Averbeck BB, Costa VD (2017) Motivational neural circuits underlying reinforcement learning. Nature neuroscience 20:505-512.

Balleine BW, Delgado MR, Hikosaka O (2007) The Role of the Dorsal Striatum in Reward and Decision-Making. The Journal of Neuroscience 27:8161-8165.

Beaulieu J-M, Gainetdinov RR (2011) The Physiology, Signaling, and Pharmacology of Dopamine Receptors. Pharmacological Reviews 63:182-217.

Berger B, Gaspar P, Verney C (1991) Dopaminergic innervation of the cerebral cortex: unexpected differences between rodents and primates. Trends Neurosci 14:21-27.

Brisch R, Saniotis A, Wolf R, Bielau H, Bernstein H-G, Steiner J, Bogerts B, Braun K, Jankowski Z, Kumaratilake J, Henneberg M, Gos T (2014) The Role of Dopamine in Schizophrenia from a Neurobiological and Evolutionary Perspective: Old Fashioned, but Still in Vogue. Frontiers in Psychiatry 5.

Brozoski TJ, Brown RM, Rosvold HE, Goldman PS (1979) Cognitive deficit caused by regional depletion of dopamine in prefrontal cortex of rhesus monkey. Science (New York, NY) 205:929-932.

Buchsbaum MS, Potkin SG, Siegel BV, Jr., Lohr J, Katz M, Gottschalk LA, Gulasekaram B, Marshall JF, Lottenberg S, Teng CY, et al. (1992) Striatal metabolic rate and clinical response to neuroleptics in schizophrenia. Archives of general psychiatry 49:966-974.

Chadick JZ, Gazzaley A (2011) Differential coupling of visual cortex with default or frontal-parietal network based on goals. Nature neuroscience 14:830-832.

Chakroun K, Mathar D, Wiehler A, Ganzer F, Peters J (2020) Dopaminergic modulation of the exploration/exploitation trade-off in human decision-making. eLife 9.

Choi JK, Chen YI, Hamel E, Jenkins BG (2006) Brain hemodynamic changes mediated by dopamine receptors: Role of the cerebral microvasculature in dopamine-mediated neurovascular coupling. NeuroImage 30:700-712.

Clarke HF, Robbins TW, Roberts AC (2008) Lesions of the medial striatum in monkeys produce perseverative impairments during reversal learning similar to those produced by lesions of the orbitofrontal cortex. The Journal of neuroscience : the official journal of the Society for Neuroscience 28:10972-10982.

Clos M, Bunzeck N, Sommer T (2019) Dopamine Enhances Item Novelty Detection via Hippocampal and Associative Recall via Left Lateral Prefrontal Cortex Mechanisms. The Journal of neuroscience : the official journal of the Society for Neuroscience 39:7920-7933.

Cohen MX (2008) Neurocomputational mechanisms of reinforcement-guided learning in humans: A review. Cognitive, Affective, & Behavioral Neuroscience 8:113-125.

Cole DM, Beckmann CF, Oei NYL, Both S, van Gerven JMA, Rombouts SARB (2013) Differential and distributed effects of dopamine neuromodulations on resting-state network connectivity. NeuroImage 78:59-67.

Cools R, D'Esposito M (2011) Inverted-U–Shaped Dopamine Actions on Human Working Memory and Cognitive Control. Biological psychiatry 69:e113-e125.

Cools R, Clark L, Robbins TW (2004) Differential responses in human striatum and prefrontal cortex to changes in object and rule relevance. The Journal of neuroscience : the official journal of the Society for Neuroscience 24:1129-1135.

Cox RW (1996) AFNI: software for analysis and visualization of functional magnetic resonance neuroimages. Computers and biomedical research, an international journal 29:162-173.

Diederen KM, Ziauddeen H, Vestergaard MD, Spencer T, Schultz W, Fletcher PC (2017) Dopamine Modulates Adaptive Prediction Error Coding in the Human Midbrain and Striatum. The Journal of neuroscience : the official journal of the Society for Neuroscience 37:1708-1720.

Eisenegger C, Naef M, Linssen A, Clark L, Gandamaneni PK, Müller U, Robbins TW (2014) Role of dopamine D2 receptors in human reinforcement learning. Neuropsychopharmacology : official publication of the American College of Neuropsychopharmacology 39:2366-2375.

Elorette C, Fujimoto A, Stoll FM, Fujimoto SH, Bienkowska N, London L, Fleysher L, Russ BE, Rudebeck PH (2024) The neural basis of resting-state fMRI functional connectivity in fronto-limbic circuits revealed by chemogenetic manipulation. Nature communications 15:4669.

Eyny YS, Horvitz JC (2003) Opposing roles of D1 and D2 receptors in appetitive conditioning. The Journal of neuroscience : the official journal of the Society for Neuroscience 23:1584-1587.

Frank MJ, Badre D (2012) Mechanisms of hierarchical reinforcement learning in corticostriatal circuits 1: computational analysis. Cerebral cortex (New York, NY : 1991) 22:509-526.

Froudist-Walsh S, Bliss DP, Ding X, Rapan L, Niu M, Knoblauch K, Zilles K, Kennedy H, Palomero-Gallagher N, Wang XJ (2021) A dopamine gradient controls access to distributed working memory in the large-scale monkey cortex. Neuron 109:3500-3520.e3513.

Fujimoto A, Elorette C, Fredericks JM, Fujimoto SH, Fleysher L, Rudebeck PH, Russ BE (2022) Resting-State fMRI-Based Screening of Deschloroclozapine in Rhesus Macaques Predicts Dosage-Dependent Behavioral Effects. The Journal of neuroscience : the official journal of the Society for Neuroscience 42:5705-5716.

Gilmore AW, Nelson SM, McDermott KB (2015) A parietal memory network revealed by multiple MRI methods. Trends in cognitive sciences 19:534-543.

Goldman RG, Alexander GE, Zemishlany Z, Mukherjee S, Sackeim HA, Prohovnik I (1996) Acute effects of haloperidol on cerebral cortex blood flow in normal and schizophrenic subjects. Biological psychiatry 40:604-608.

Grayson DS, Bliss-Moreau E, Machado CJ, Bennett J, Shen K, Grant KA, Fair DA, Amaral DG (2016) The Rhesus Monkey Connectome Predicts Disrupted Functional Networks Resulting from Pharmacogenetic Inactivation of the Amygdala. Neuron 91:453-466.

Hartig R, Glen D, Jung B, Logothetis NK, Paxinos G, Garza-Villarreal EA, Messinger A, Evrard HC (2021) The Subcortical Atlas of the Rhesus Macaque (SARM) for neuroimaging. NeuroImage 235:117996.

Hori Y, Nagai Y, Mimura K, Suhara T, Higuchi M, Bouret S, Minamimoto T (2021) D1- and D2-like receptors differentially mediate the effects of dopaminergic transmission on cost-benefit evaluation and motivation in monkeys. PLoS biology 19:e3001055.

Hwang J, Mitz AR, Murray EA (2019) NIMH MonkeyLogic: Behavioral control and data acquisition in MATLAB. Journal of neuroscience methods 323:13-21.

Ishiwata K, Oda K, Sakata M, Kimura Y, Kawamura K, Oda K, Sasaki T, Naganawa M, Chihara K, Okubo Y, Ishii K (2006) A feasibility study of [11C]SA4503-PET for evaluating sigmal receptor occupancy by neuroleptics: the binding of haloperidol to sigma1 and dopamine D2-like receptors. Annals of nuclear medicine 20:569-573.

Jenni NL, Li YT, Floresco SB (2021) Medial orbitofrontal cortex dopamine D(1)/D(2) receptors differentially modulate distinct forms of probabilistic decision-making. Neuropsychopharmacology : official publication of the American College of Neuropsychopharmacology 46:1240-1251.

Jocham G, Klein TA, Ullsperger M (2011) Dopamine-Mediated Reinforcement Learning Signals in the Striatum and Ventromedial Prefrontal Cortex Underlie Value-Based Choices. The Journal of Neuroscience 31:1606-1613.

Jung B, Taylor PA, Seidlitz J, Sponheim C, Perkins P, Ungerleider LG, Glen D, Messinger A (2021) A comprehensive macaque fMRI pipeline and hierarchical atlas. NeuroImage 235:117997.

Kahnt T, Weber SC, Haker H, Robbins TW, Tobler PN (2015) Dopamine D2-receptor blockade enhances decoding of prefrontal signals in humans. The Journal of neuroscience : the official journal of the Society for Neuroscience 35:4104-4111.

677 Kapur S, Wadenberg ML, Remington G (2000) Are animal studies of antipsychotics appropriately dosed? Lessons
678 from the bedside to the bench. Canadian journal of psychiatry Revue canadienne de psychiatrie 45:241-
679 246.
680 Kassebaum P (2023) circularGraph (https://github.com/paul-kassebaum-mathworks/circularGraph), GitHub. .
681 Kohno M, Morales AM, Ghahremani DG, Hellemann G, London ED (2014) Risky decision making, prefrontal
682 cortex, and mesocorticolimbic functional connectivity in methamphetamine dependence. JAMA
683 psychiatry 71:812-820.
684 Kunimatsu J, Tanaka M (2016) Striatal dopamine modulates timing of self-initiated saccades. Neuroscience
685 337:131-142.
686 Lako IM, van den Heuvel ER, Knegtering H, Bruggeman R, Taxis K (2013) Estimating dopamine D_2 receptor
687 occupancy for doses of 8 antipsychotics: a meta-analysis. Journal of clinical psychopharmacology
688 33:675-681.
689 Li N, Ma N, Liu Y, He XS, Sun DL, Fu XM, Zhang X, Han S, Zhang DR (2013) Resting-state functional connectivity
690 predicts impulsivity in economic decision-making. The Journal of neuroscience : the official journal of the
691 Society for Neuroscience 33:4886-4895.
692 Lidow MS, Williams GV, Goldman-Rakic PS (1998) The cerebral cortex: a case for a common site of action of
693 antipsychotics. Trends in pharmacological sciences 19:136-140.
694 Lim HS, Kim SJ, Noh YH, Lee BC, Jin SJ, Park HS, Kim S, Jang IJ, Kim SE (2013) Exploration of optimal dosing
695 regimens of haloperidol, a D2 Antagonist, via modeling and simulation analysis in a D2 receptor
696 occupancy study. Pharmaceutical research 30:683-693.
697 Mizrahi R, Rusjan P, Agid O, Graff A, Mamo DC, Zipursky RB, Kapur S (2007) Adverse subjective experience with
698 antipsychotics and its relationship to striatal and extrastriatal D2 receptors: a PET study in schizophrenia.
699 The American journal of psychiatry 164:630-637.
700 Mukherjee J, Christian BT, Narayanan TK, Shi B, Mantil J (2001) Evaluation of dopamine D-2 receptor occupancy
701 by clozapine, risperidone, and haloperidol in vivo in the rodent and nonhuman primate brain using 18F-
702 fallypride. Neuropsychopharmacology : official publication of the American College of
703 Neuropsychopharmacology 25:476-488.
704 Murray EA, Rudebeck PH (2018) Specializations for reward-guided decision-making in the primate ventral
705 prefrontal cortex. Nature reviews Neuroscience 19:404-417.
706 Narendran R, Jedema HP, Lopresti BJ, Mason NS, Gurnsey K, Ruszkiewicz J, Chen CM, Deuitch L, Frankle WG,
707 Bradberry CW (2014) Imaging dopamine transmission in the frontal cortex: a simultaneous microdialysis
708 and [11C]FLB 457 PET study. Molecular psychiatry 19:302-310.
709 Narendran R, Frankle WG, Mason NS, Rabiner EA, Gunn RN, Searle GE, Vora S, Litschge M, Kendro S, Cooper TB,
710 Mathis CA, Laruelle M (2009) Positron emission tomography imaging of amphetamine-induced
711 dopamine release in the human cortex: a comparative evaluation of the high affinity dopamine D2/3
712 radiotracers [11C]FLB 457 and [11C]fallypride. Synapse (New York, NY) 63:447-461.
713 Noudoost B, Moore T (2011) Control of visual cortical signals by prefrontal dopamine. Nature 474:372-375.
714 Ott T, Nieder A (2019) Dopamine and Cognitive Control in Prefrontal Cortex. Trends in cognitive sciences 23:213-
715 234.
716 Pessiglione M, Seymour B, Flandin G, Dolan RJ, Frith CD (2006) Dopamine-dependent prediction errors underpin
717 reward-seeking behaviour in humans. Nature 442:1042-1045.
718 Puig MV, Miller EK (2012) The role of prefrontal dopamine D1 receptors in the neural mechanisms of associative
719 learning. Neuron 74:874-886.
720 Puig MV, Miller EK (2015) Neural Substrates of Dopamine D2 Receptor Modulated Executive Functions in the
721 Monkey Prefrontal Cortex. Cerebral cortex (New York, NY : 1991) 25:2980-2987.
722 Raghanti MA, Stimpson CD, Marcinkiewicz JL, Erwin JM, Hof PR, Sherwood CC (2008) Cortical dopaminergic
723 innervation among humans, chimpanzees, and macaque monkeys: A comparative study. Neuroscience
724 155:203-220.

Remy P, Samson Y (2003) The role of dopamine in cognition: evidence from functional imaging studies. Current Opinion in Neurology 16:S37-S41.

Robbins TW, Everitt BJ (2002) Dopamine — Its Role in Behaviour and Cognition in Experimental Animals and Humans. In: Dopamine in the CNS II (Di Chiara G, ed), pp 173-211. Berlin, Heidelberg: Springer Berlin Heidelberg.

Rudebeck PH, Saunders RC, Lundgren DA, Murray EA (2017a) Specialized Representations of Value in the Orbital and Ventrolateral Prefrontal Cortex: Desirability versus Availability of Outcomes. Neuron 95:1208-1220.e1205.

Rudebeck PH, Ripple JA, Mitz AR, Averbeck BB, Murray EA (2017b) Amygdala contributions to stimulus–reward encoding in the macaque medial and orbital frontal cortex during learning. Journal of neuroscience 37:2186-2202.

Sawaguchi T, Goldman-Rakic PS (1991) D1 dopamine receptors in prefrontal cortex: involvement in working memory. Science (New York, NY) 251:947-950.

Schultz W, Dayan P, Montague PR (1997) A Neural Substrate of Prediction and Reward. Science (New York, NY) 275:1593-1599.

Sedvall GC, Karlsson P (1999) Pharmacological Manipulation of D1-Dopamine Receptor Function in Schizophrenia. Neuropsychopharmacology : official publication of the American College of Neuropsychopharmacology 21:S181-S188.

Seeman P (1987) Dopamine receptors and the dopamine hypothesis of schizophrenia. Synapse (New York, NY) 1:133-152.

Seidlitz J, Sponheim C, Glen D, Ye FQ, Saleem KS, Leopold DA, Ungerleider L, Messinger A (2018) A population MRI brain template and analysis tools for the macaque. NeuroImage 170:121-131.

Self DW (2010) Dopamine Receptor Subtypes in Reward and Relapse. In: The Dopamine Receptors (Neve KA, ed), pp 479-524. Totowa, NJ: Humana Press.

Sescousse G, Caldú X, Segura B, Dreher J-C (2013) Processing of primary and secondary rewards: A quantitative meta-analysis and review of human functional neuroimaging studies. Neuroscience & Biobehavioral Reviews 37:681-696.

Settle EC, Jr., Ayd FJ, Jr. (1983) Haloperidol: a quarter century of experience. The Journal of clinical psychiatry 44:440-448.

St Onge JR, Abhari H, Floresco SB (2011) Dissociable contributions by prefrontal D1 and D2 receptors to risk-based decision making. The Journal of neuroscience : the official journal of the Society for Neuroscience 31:8625-8633.

Suhara T, Sudo Y, Okauchi T, Maeda J, Kawabe K, Suzuki K, Okubo Y, Nakashima Y, Ito H, Tanada S, Halldin C, Farde L (1999) Extrastriatal dopamine D2 receptor density and affinity in the human brain measured by 3D PET. The international journal of neuropsychopharmacology 2:73-82.

Suhara T, Okubo Y, Yasuno F, Sudo Y, Inoue M, Ichimiya T, Nakashima Y, Nakayama K, Tanada S, Suzuki K, Halldin C, Farde L (2002) Decreased dopamine D2 receptor binding in the anterior cingulate cortex in schizophrenia. Archives of general psychiatry 59:25-30.

Sutton RS, Barto AG (1981) Toward a modern theory of adaptive networks: expectation and prediction. Psychological review 88:135.

Takahashi H, Yamada M, Suhara T (2012) Functional significance of central D1 receptors in cognition: beyond working memory. Journal of cerebral blood flow and metabolism : official journal of the International Society of Cerebral Blood Flow and Metabolism 32:1248-1258.

Taylor PA, Saad ZS (2013) FATCAT: (an efficient) Functional and Tractographic Connectivity Analysis Toolbox. Brain connectivity 3:523-535.

Tritsch Nicolas X, Sabatini Bernardo L (2012) Dopaminergic Modulation of Synaptic Transmission in Cortex and Striatum. Neuron 76:33-50.

Tsukada H, Nishiyama S, Fukumoto D, Sato K, Kakiuchi T, Domino EF (2005) Chronic NMDA antagonism impairs working memory, decreases extracellular dopamine, and increases D1 receptor binding in prefrontal cortex of conscious monkeys. Neuropsychopharmacology : official publication of the American College of Neuropsychopharmacology 30:1861-1869.

van der Meer MA, Redish AD (2011) Ventral striatum: a critical look at models of learning and evaluation. Current opinion in neurobiology 21:387-392.

Vancraeyenest P, Arsenault JT, Li X, Zhu Q, Kobayashi K, Isa K, Isa T, Vanduffel W (2020) Selective Mesoaccumbal Pathway Inactivation Affects Motivation but Not Reinforcement-Based Learning in Macaques. Neuron 108:568-581.e566.

Vo K, Rutledge RB, Chatterjee A, Kable JW (2014) Dorsal striatum is necessary for stimulus-value but not action-value learning in humans. Brain : a journal of neurology 137:3129-3135.

Vogelsang DA, Furman DJ, Nee DE, Pappas I, White RL, III, Kayser AS, D'Esposito M (2023) Dopamine Modulates Effective Connectivity in Frontal Cortex. Journal of cognitive neuroscience:1-11.

Volkow ND, Gur RC, Wang GJ, Fowler JS, Moberg PJ, Ding YS, Hitzemann R, Smith G, Logan J (1998) Association between decline in brain dopamine activity with age and cognitive and motor impairment in healthy individuals. The American journal of psychiatry 155:344-349.

Wang M, Vijayraghavan S, Goldman-Rakic PS (2004) Selective D2 receptor actions on the functional circuitry of working memory. Science (New York, NY) 303:853-856.

Wang X, Li XH, Cho JW, Russ BE, Rajamani N, Omelchenko A, Ai L, Korchmaros A, Sawiak S, Benn RA, Garcia-Saldivar P, Wang Z, Kalin NH, Schroeder CE, Craddock RC, Fox AS, Evans AC, Messinger A, Milham MP, Xu T (2021) U-net model for brain extraction: Trained on humans for transfer to non-human primates. NeuroImage 235:118001.

White JK, Monosov IE (2016) Neurons in the primate dorsal striatum signal the uncertainty of object–reward associations. Nature communications 7:12735.

Yael D, Zeef D, Sand D, Moran A, Katz D, Cohen D, Temel Y, Bar-Gad I (2013) Haloperidol-induced changes in neuronal activity in the striatum of the freely moving rat. Frontiers in systems neuroscience 7.

Yun S, Yang B, Anair JD, Martin MM, Fleps SW, Pamukcu A, Yeh NH, Contractor A, Kennedy A, Parker JG (2023) Antipsychotic drug efficacy correlates with the modulation of D1 rather than D2 receptor-expressing striatal projection neurons. Nature neuroscience 26:1417-1428.

Zeeb FD, Robbins TW, Winstanley CA (2009) Serotonergic and dopaminergic modulation of gambling behavior as assessed using a novel rat gambling task. Neuropsychopharmacology : official publication of the American College of Neuropsychopharmacology 34:2329-2343.

Zipursky RB, Christensen BK, Daskalakis Z, Epstein I, Roy P, Furimsky I, Sanger T, Kapur S (2005) Treatment response to olanzapine and haloperidol and its association with dopamine D receptor occupancy in first-episode psychosis. Canadian journal of psychiatry Revue canadienne de psychiatrie 50:462-469.

Subject	*Behavior*	*SCH-rsMRI*	*HAL-rsMRI*	*Saline-rsMRI*
Ee	Y	Y	N	Y
Me	Y	N	Y	N
Pi	Y	Y	Y	Y
St	Y	Y	Y	N
Bu	N	N	N	Y
Cy	N	N	N	Y
Wo	N	N	N	Y

Table 1. Assignments of monkeys to resting-state fMRI and behavioral testing conditions. Y and N indicate the condition that the data was collected and not collected, respectively. SCH: SCH-23390 (10 µg/kg), HAL: haloperidol (50 µg/kg). Note that animals assigned to behavioral experiments (Ee, Me, Pi, St) went through all drug treatment conditions.

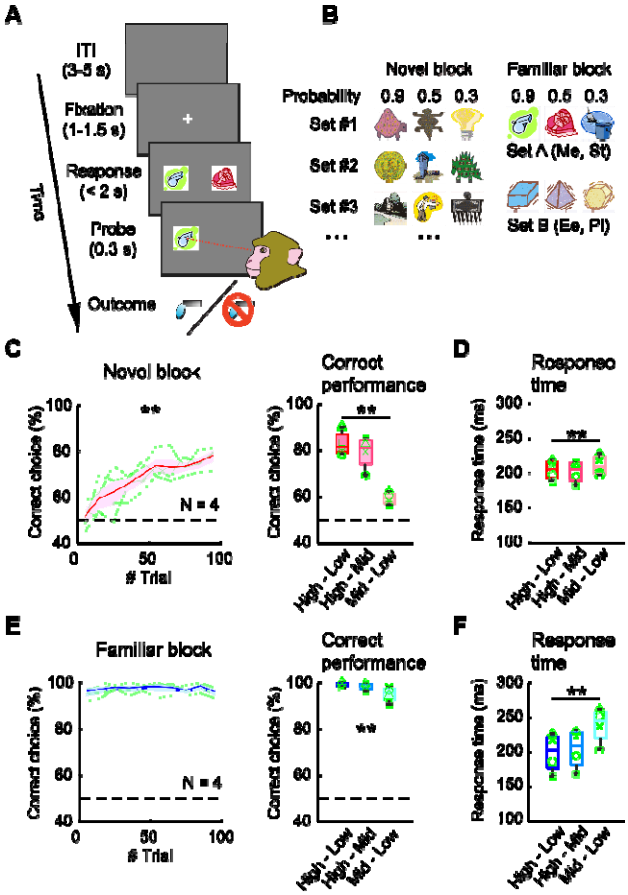

Figure 1. Behavioral task and baseline behavioral performance. (**A**) Trial sequence. Animals were required to respond to one of two visual stimuli on the screen by eye movement to acquire a drop of juice. (**B**) Stimulus sets. Stimuli were pictures that were associated with different reward probabilities (0.9, 0.5, 0.3). In novel blocks (left), a new set of three pictures was used in each block. In familiar blocks (right), a fixed set of pictures was prepared for each monkey and used repeatedly throughout the experiment. (**C**) Task performance in novel blocks. Correct performance was gradually increased over trials in a block (left) and depending on which stimuli were paired in the trial (right). Dashed lines indicate chance level, and the plots show mean and standard error. Green lines indicate the average performance of each animal. Box plots indicate the median, 25th and 75th percentiles, and the extent of data points obtained in the 2nd half of each block. High-Low: 0.9-0.3, High-Mid: 0.9-0.5, Mid-Low: 0.5-0.3. Symbols indicate individual animals. (**D**) Response time (RT) in novel blocks reflected reward probability of the stimulus pair. (**E and F**) Behaviors in familiar blocks. Correct performance was stable throughout the block. Performance and RT reflected reward probability. Conventions are the same as **C-D**. ** $p < 0.01$, interaction of trial bin by block type, 2-way repeated-measures ANOVA, or main effect of stimulus pair, 1-way repeated-measures ANOVA.

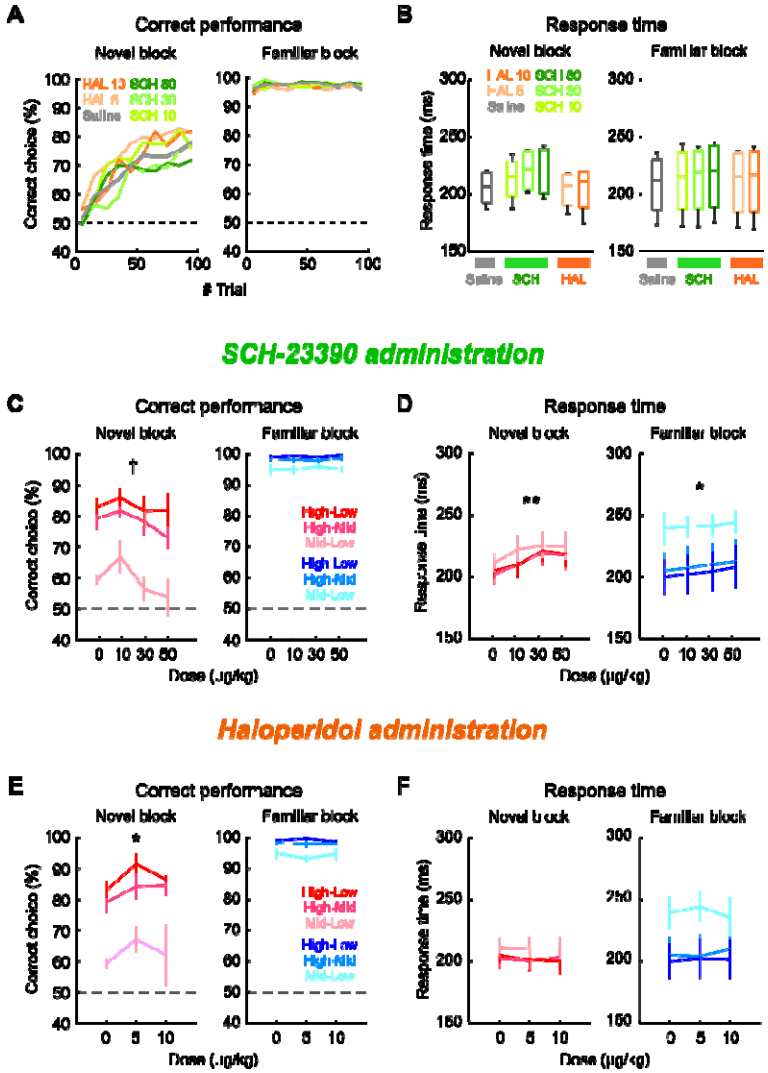

Figure 2. Effects of DA receptor antagonists on behaviors. (**A-B**) Overall summary of drug effects on behaviors. (**A**) Averaged performance (proportion of correct choice) plotted against the trial number for novel (left) and familiar (right) blocks, respectively. Line colors indicate the drug type and shade indicates the dose, orange shades (Haloperidol), green shades (SCH-23390), grey (Saline). (**B**) Drug effects on response time (RT). Box plots indicate the median, 25th and 75th percentiles, and the extent of data points. (**C-F**) Drug effects collapsed by drug dose and stimulus pair. (**C**) Task performance in SCH-23390 sessions. Correct performance tended to decrease when higher dose of SCH was administered in novel blocks (left) but did not change in familiar blocks (right). The colors of lines indicate stimulus pairs. (**D**) RT in SCH-23390 sessions. RT increased following SCH injection. (**E and F**) Haloperidol sessions. Conventions are the same as **C-D**. †p < 0.10, *p < 0.05, **p < 0.01, 2-way repeated-measures ANOVA. Symbols indicate individual animals.

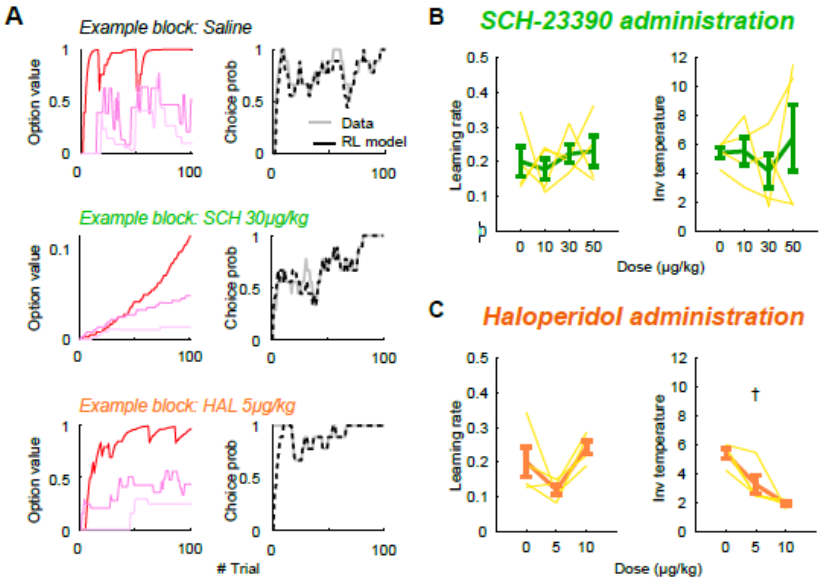

Figure 3: Reinforcement learning model fitting. (**A**) RL model fitting on choice data in an example block with administration of saline (top), SCH-23390 (middle), and haloperidol (bottom). The left panels show the transition of the model estimated value in example blocks (line colors indicate stimuli). The right panels show the animal's choice probability (gray solid lines) and the estimated choice probability based on RL model (black broken lines) in the same blocks. (**B**) The dose-dependent effects of SCH-23390 on learning rate (left) and inverse temperature (right). Thin yellow lines indicate the data from individual animals. (**C**) The dose-dependent effects of haloperidol on learning rate (left) and inverse temperature (right). †$p < 0.10$.

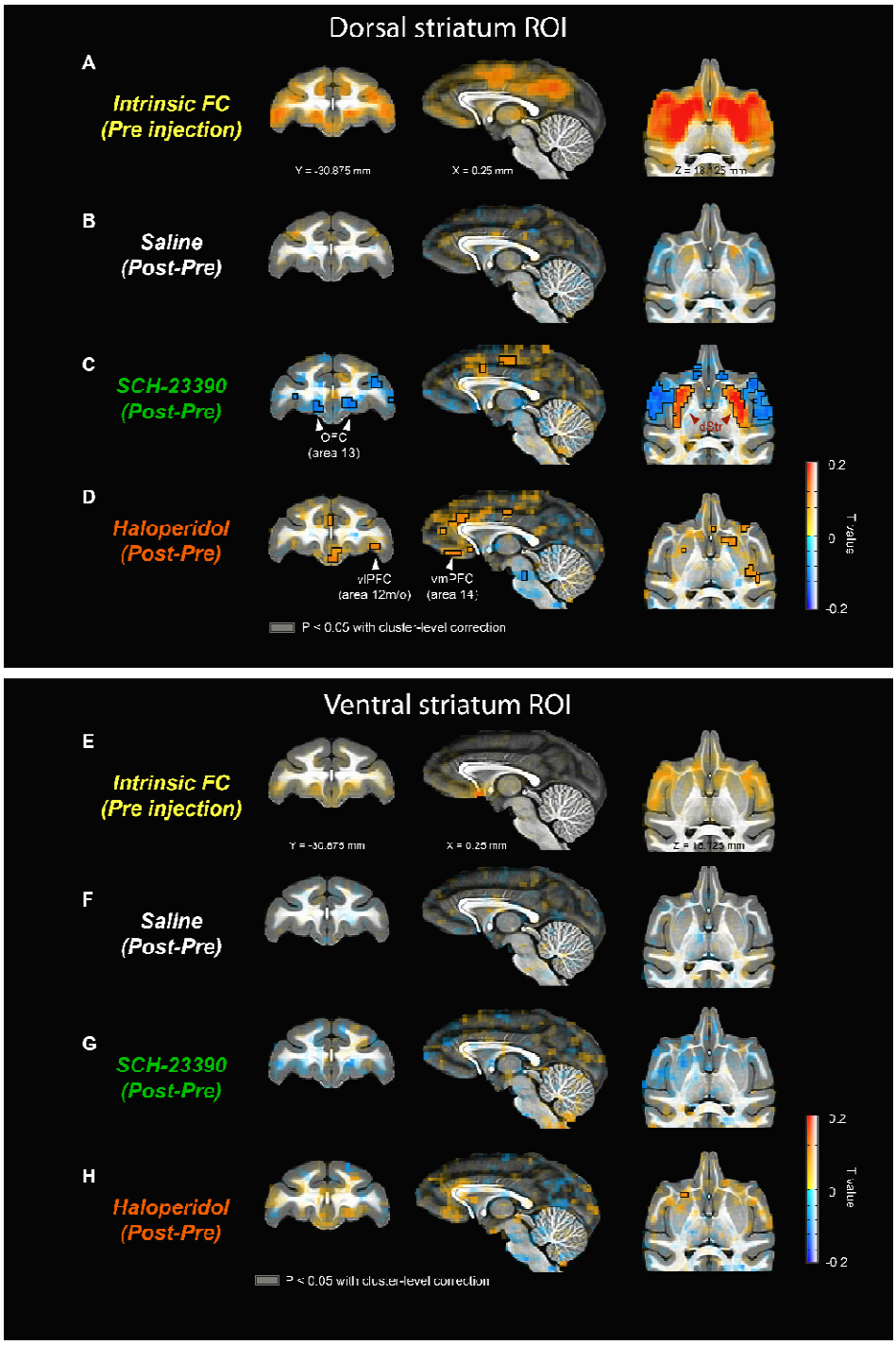

Figure 4. Functional connectivity analysis. (**A**) Whole-brain FC computed using dorsal striatum as ROI to pre-injection images. Coronal (left), sagittal (middle), and axial planes (right) are shown. Colors indicate strength of FC (T-value). (**B**) Changes in dorsal striatum FC from pre- to post-saline injection scans. (**C**) SCH-23390 effects on FC. (**D**) Haloperidol effects on FC. The voxels enclosed in black lines are the clusters with a significant change in dorsal striatum FC ($p < 0.05$, cluster-level correction). Note that the statistical tests were performed only for subtraction images in **B-D**. dStr: dorsal striatum, OFC: orbitofrontal cortex, vlPFC: ventrolateral prefrontal cortex, vmPFC: ventromedial prefrontal cortex. (**E-**

H) Whole-brain FC changes computed using ventral striatum as ROI. Conventions are the same as in **A-D**.

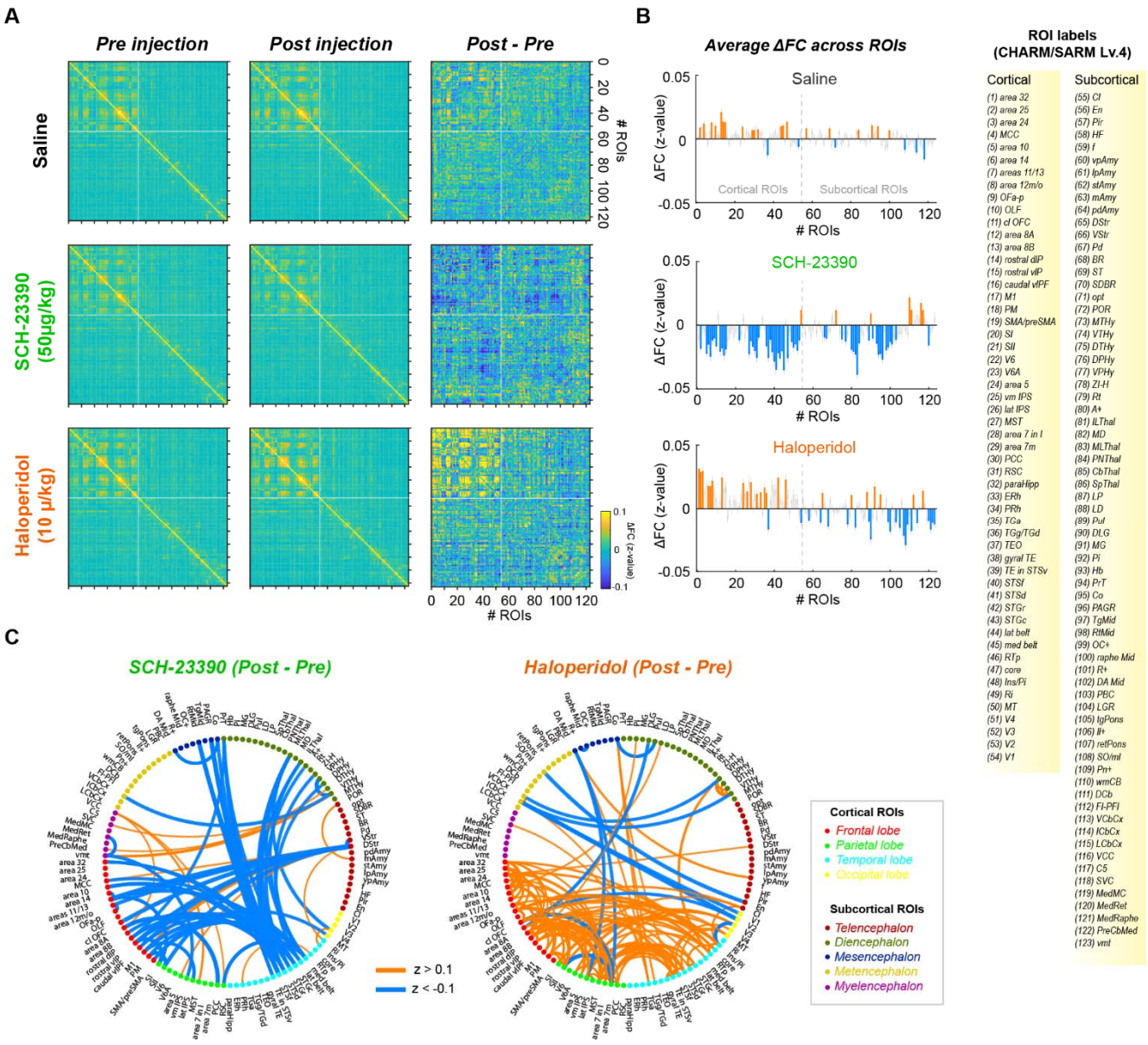

Figure 5. Connectome analysis. (**A**) Connectome for pre-injection (left), post-injection (middle), and their difference (ΔFC, right) are shown for sessions with injection of saline (top row), SCH-23390 (middle row), and haloperidol (bottom row), respectively. X and Y axes are the number of ROIs defined by macaque brain hierarchical atlas (CHARM/SARM atlas at level 4). Colors indicate the FC of each pair of ROIs (z-value). White lines on connectome divide cortical and subcortical ROIs. (**B**) Bar plots showing average ΔFC for saline (top), SCH-23390 (middle), and haloperidol (bottom) sessions. ΔFC (z-value) is averaged for each ROI. Orange and blue bars indicate significant ΔFC from zero ($p < 0.05$, Bonferroni correction). Dashed lines divide cortical and subcortical ROIs. ROI labels from CHARM/SARM level 4 are shown on the right. (**C**) Circular plots depicting the effects of injection of SCH-23390 (left) or haloperidol (right) on the whole-brain FC. Seed region labels correspond to ROI labels in **B**. The changes in FC are indicated by color (orange: positive changes, blue: negative changes) and width of lines (absolute z-value changes > 0.1). The color of each seed indicates the region defined by CHARM/SARM level 1 (inset).

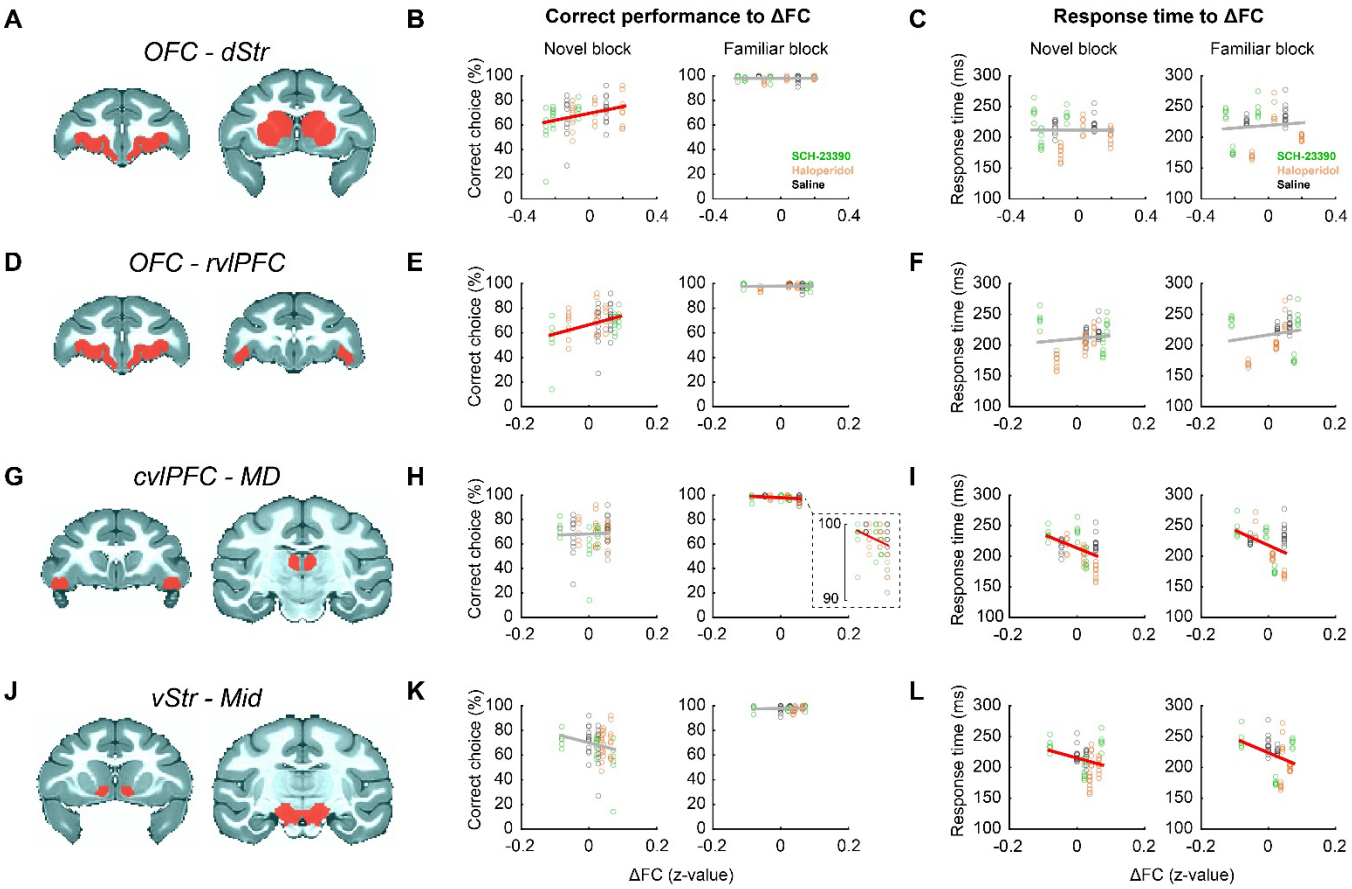

Figure 6. Direct comparison of behaviors and resting-state FC. (**A-C**) Correlation between orbitofrontal cortex to dorsal striatum ΔFC and task performance in novel (left) and familiar (right) blocks (**B**) or response time (**C**). Red areas in brain map show bilateral ROIs. Plots indicate behavioral data and corresponding ΔFC in saline (black), SCH-23390 (green), and haloperidol (orange) sessions. Red and gray lines on scatter plots indicate significant ($p < 0.05$, linear regression analysis) and non-significant relationships between behavior and ΔFC, respectively. (**D-F**) Correlation between orbitofrontal cortex to rostral part of ventrolateral prefrontal cortex ΔFC and behaviors. (**G-I**) Correlation between the caudal part of ventrolateral prefrontal cortex to mediodorsal thalamus ΔFC and behaviors. Inset is a magnification image for the correlation between familiar block performance and ΔFC. (**J-L**) Correlation between ventral striatum to midbrain ΔFC and behaviors. Conventions are the same as **A-C**.

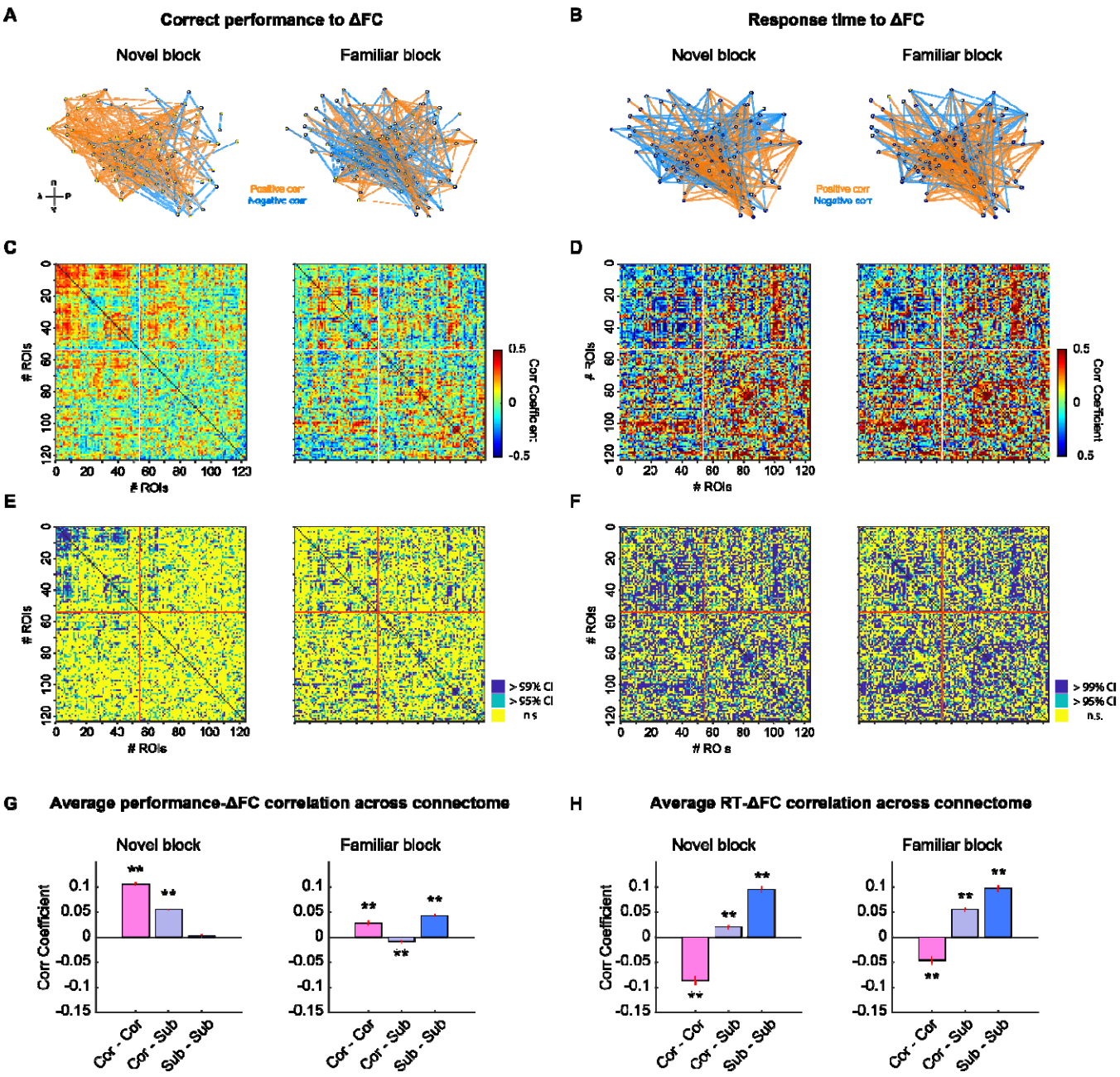

Figure 7. Whole-brain network correlation to behaviors across all drug conditions. (**A**) Strength of performance-ΔFC correlation projected into brain map. The top 5% of connections that showed strong behavior-ΔFC correlation are visualized. Black dots indicate the center of mass of ROIs. The strength and direction of changes in FC are depicted as the width and color (orange: positive, blue: negative) of lines, respectively. (**B**) Strength of RT-ΔFC correlation projected into brain map. (**C**) Correlation matrix depicting relationship between changes in FC and task performance in novel (left) and familiar (right) blocks. The ROIs used are the same as in **Fig. 5A**. Colors indicate performance-ΔFC correlation coefficient. (**D**) Correlation between changes in FC and RT. (**E and F**) Functional connections (ROI pairs) that showed a significant correlation between FC changes and correct performance (**E**) or RT (**F**) (> 95% CI, permutation test) are shown in the matrix used in **C-D**. (**G**) Bar plots depicting average performance-ΔFC correlation coefficients calculated for cortico-cortical, cortico-subcortical, and

subcortico-subcortical connections separately, in novel (left panel) and familiar (right panel) blocks. (**H**) Averaged correlation coefficients for RT to ΔFC. **$p < 0.01$, rank-sum test.

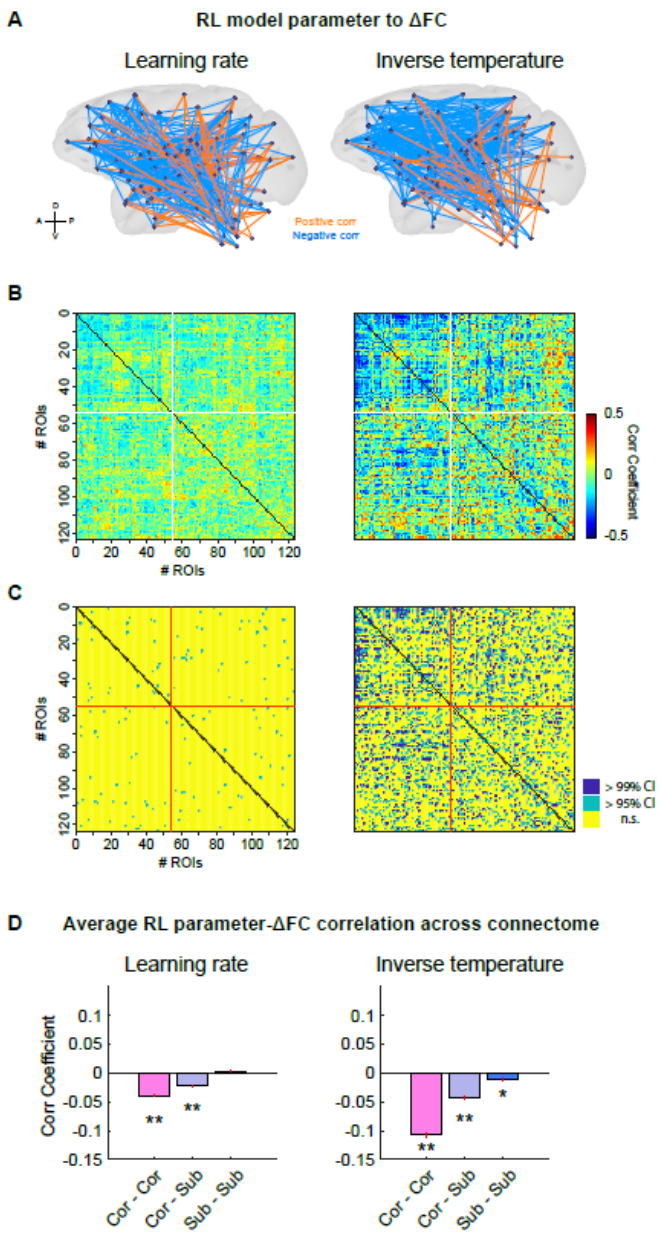

Figure 8. Whole-brain network correlation to reinforcement learning-model parameters across all drug conditions. (**A**) Strength of RL model parameters-ΔFC correlation projected into a brain map (Left: learning rate, right: inverse temperature). The strength and direction of changes in FC (top 5% of connections) are depicted as the width and color of lines (orange: positive, blue: negative) respectively. (**B**) Correlation matrix depicting the relationship between changes in FC and RL model parameters. Colors indicate RL model parameter-ΔFC correlation coefficient. (**C**) Functional connections (ROI pairs) that showed a significant correlation between FC changes and RL parameters (> 95% CI, permutation test) are shown in the matrix used in **B**. (**D**) Bar plots depicting average RL model parameters-ΔFC correlation coefficients calculated for cortico-cortical, cortico-subcortical, and subcortico-subcortical connections separately. **p < 0.01, rank-sum test. Conventions are the same as **Fig. 7**.